

Do uniform tangential interfacial stresses enhance adhesion?

Nicola Menga^{1,3}, Giuseppe Carbone^{1,2,3}, Daniele Dini^{1,3}

¹*Department of Mechanics, Mathematics and Management,
Politecnico di Bari, v.le Japigia 182, 70126 Bari - Italy*

²*Physics Department M. Merlin, CNR Institute for Photonics and
Nanotechnologies U.O.S. Bari via Amendola 173, 70126 Bari, Italy and*

³*Department of Mechanical Engineering,
Imperial College London, South Kensington Campus,
Exhibition Road London SW7 2AZ, United Kingdom*

Abstract

We present theoretical arguments, based on linear elasticity and thermodynamics, to show that interfacial tangential stresses in sliding adhesive soft contacts may lead to a significant increase of the effective energy of adhesion. A sizable expansion of the contact area is predicted in conditions corresponding to such scenario. These results are easily explained and are valid under the assumptions that: (i) sliding at the interface does not lead to any loss of adhesive interaction and (ii) spatial fluctuations of frictional stresses can be considered negligible. Our results are seemingly supported by existing experiments, and shows that frictional stress may lead to a reduction or to an increase of the effective energy of adhesion depending on which conditions are established at the interface of contacting bodies in the presence of adhesive forces.

I. INTRODUCTION

In the last decades, contact mechanics, and in particular the effect of physical interactions occurring at the interface between elastic and viscoelastic solids, has found increasing scientific interest, mostly boosted by practical applications, such as tires, seals, bio-inspired climbing robots, and adhesive gloves. The contact behavior of such systems has been studied by many authors relying on different approaches: analytical techniques [1–7], advanced numerical simulations [8–15] and experimental investigations [16–20].

Among the many factors influencing interactions occurring in contact problems, the interplay between shear stresses (and associated frictional response) and adhesion in elastic contacts is a long-standing tribological problem. Many authors have contributed to shed light on the relation between friction, adhesion and contact area, motivated by the relevance that this phenomenon has in a countless number of engineering applications involving *e.g.* wear [21–24], shear resistance [25, 26], tire friction [27, 28], electric resistance [31], mixed and boundary lubrication [32, 33], and slippery prosthetic devices [29, 30]. Therefore, both experimental [34–36, 38] and theoretical investigations [34, 37] have been carried out on this specific topic with the aim of providing additional insights into the adhesive behavior of frictional contacts. In particular, most of them seem to indicate that the presence of relative sliding and friction at the interface always leads to a reduction of the contact area, and, therefore weakens the adhesion strength. This phenomenon, which is known as a friction induced transition from the adhesive JKR regime [41] to the adhesiveless Hertz regime, is usually explained by relying on the arguments presented firstly by Savkoor and Briggs [34], and then by Johnson [37]. However, we cannot ignore the fact that the theoretical arguments presented in Ref. [34] holds true only for the case of contacts in the presence of full stick between the meeting surfaces, where the occurrence of slip at the contact interface is prevented from taking place (*i.e.* in the presence of uniform tangential displacement). Therefore, this theory is not well suited to deal with sliding contacts as those addressed in Refs [35, 36, 38–40], where gross slip conditions between almost perfectly smooth surfaces are investigated, leading to significantly different conclusions: the presence of slip at moderate velocities does not lead to any reduction of contact area, and in some cases, as clearly observed in Refs. [39, 40], may even lead to an increase of the contact area. Moderate slip velocities, then, do not hinder adhesion. A loss of adhesion is instead observed at higher sliding velocities, and is often related to stick-slip transitions. However, even the loss of adhesion observed at high velocity, cannot be explained with the no-slip Savkoor and Briggs’ theory, where the presence of the tangential stress singularity at the edge of the contact makes the energy release rate increase, weakens the adhesive bond and leads to a decrease of the contact area. On the contrary, in presence of gross slip at the interface, the tangential stresses singularity is prevented from occurring, thus impeding the mechanism described by Savkoor and Briggs [34] from taking place. From the theoretical point of view, every existing attempt at showing the relationship between shear and adhesion has overlooked this aspect of the problem (see *e.g.* [37, 44]). In gross slip, a first possible mechanism of adhesion loss has been described firstly by Schallamach [42] and then by Chernyak and Leonov [43], where the loss of adhesion can be attributed to breaking and partial reformation of adhesive bonds during sliding. A second mechanism could be, instead, related to the effect of spatial frictional stress fluctuations and the interface, which as we shown in the paper, lead to an additional repulsive surface energy term, which may counterbalance the adhesion forces. Unfortunately, to the best of our knowledge, experimental evidence aimed at shedding light

on this is lacking, and this is mainly due to the fact that investigations in the regime of interest require very accurate instrumentation and analytical techniques.

In this study, we focus on adhesive sliding contacts between perfectly smooth surfaces under the condition that gross slip takes place at moderate velocities. We treat the exemplar case of a smooth rigid sphere sliding on a soft elastic half-space, and present a rigorous thermodynamic treatment of the contact behavior at the interface aimed at deepening the understanding of the influence of tangential stresses on adhesion and contact area. We have spent much time investigating this peculiar and yet under-investigated phenomenon, supported by the theoretical results presented in this contribution and by a novel interpretation of the few existing experimental results reported in the literature on this topic.

II. FORMULATION

We consider the case of an elastic half-space in sliding contact with a spherical rigid indenter of radius R , as shown in Fig. 1. As a result of the contact interactions, the half-space is loaded with a certain distribution of normal and tangential stresses on a portion Ω of its surface (namely the contact domain). In particular, we focus on the specific case where the tangential stress at the interface are uniformly distributed with value τ . This choice is strictly related to the observation that in sliding contacts of soft polymeric materials the interfacial tangential stresses do not follow a Coulomb friction law but rather they are almost uniform at the interface [45, 46].

For the system at hand (see Fig. 1), we define as $u(\mathbf{x})$ and $v(\mathbf{x})$ the normal and tangential displacement fields respectively.

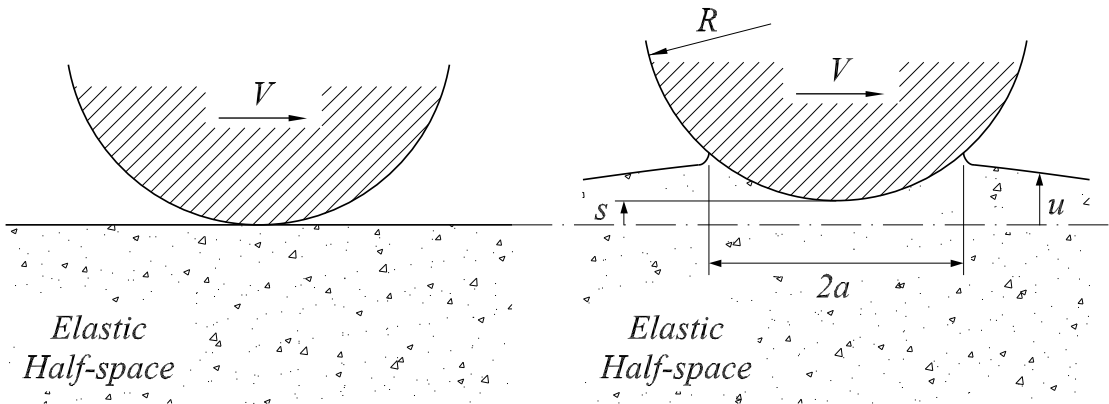


FIG. 1: The geometrical scheme of the contact problem: a rigid spherical indenter of radius R is sliding at constant velocity V over an elastic half-space. In the figure, a is the contact area radius, and s is the contact separation.

Recalling that the tangential stresses are uniformly distributed on the contact area, the elastic energy stored in the body can be calculated as

$$\mathcal{E} = \frac{1}{2} \int_{\Omega} d^2x \sigma(\mathbf{x}) u(\mathbf{x}) + \frac{1}{2} \tau W, \quad (1)$$

where Ω is the contact domain, and the quantity

$$W = \int_{\Omega} d^2x v(\mathbf{x}) = v_m A \quad (2)$$

is, what we call, the *displaced tangential volume*, being v_m the average tangential displacement in the contact area. The internal energy of the system is then given by

$$\mathcal{U}(s, W, A) = \mathcal{E}(s, W, A) - \Delta\gamma A, \quad (3)$$

where $\Delta\gamma$ work of adhesion and $A = |\Omega|$ is the contact area. Finding the minimum of $\mathcal{U}(s, W, A)$ allows to find the contact solution when the state parameters are the separation s (or equivalently the penetration $\delta = -s$), the tangentially displaced volume W , and the contact area A . However, in our problem, the state variables are (s, τ, A) , as the shear stress τ is uniform in the contact area and is actually kept constant as the system configuration changes towards the final equilibrium state. In such a case, there is a certain amount of mechanical energy associated with the constant stress field τ . Therefore, the right thermodynamic potential must consider the potential energy associated with the uniformly distributed stress τ and can be determined by performing the following Legendre transform (see [58]):

$$\mathcal{H} = \mathcal{U} - \left(\frac{\partial \mathcal{U}}{\partial W} \right)_{s,A} W = \mathcal{U} - \tau W, \quad (4)$$

where, in fact, the term $-\tau W$ is the potential energy associated with the uniform stress distribution τ . This leads to define the new thermodynamic potential

$$\mathcal{H}(s, \tau, A) = \frac{1}{2} \int_D d^2x \sigma(\mathbf{x}) u(\mathbf{x}) - \frac{1}{2} \tau W - \Delta\gamma A. \quad (5)$$

Minimizing $\mathcal{H}(s, \tau, A)$ at fixed separation s and shear stress τ , implies that

$$\left(\frac{\partial \mathcal{H}}{\partial A} \right)_{s,\tau} = 0. \quad (6)$$

Equation (6) allows to find the equilibrium solution of the system. Furthermore, we note that

$$\left(\frac{\partial \mathcal{H}}{\partial s} \right)_{A,\tau} = F, \quad (7)$$

where F is the total remote tractive force acting on the sphere.

In what follows we consider the case of soft polymeric materials. We assume that the material is incompressible (Poisson's ratio $\nu = 0.5$), which makes the tangential and normal elastic fields uncoupled, and that the elastic substrate is a half-space, in contact with a rigid sphere of radius R , over a circular area of radius $a \ll R$ (see figure 1b). The displaced tangential volume is $W = \pi a^2 v_m$, where v_m can be easily estimated by observing that tangential strain must be of order v_m/a . Therefore, because of linear elasticity, being G the shear modulus, the tangential stress τ must be of order Gv_m/a , which gives

$$v_m = K \frac{\tau}{G} a, \quad (8)$$

with K being a constant of order unity. Equation (8) can be also obtained by dimensional arguments [48–50]. Recalling the Gibbs phase rule [51], there must be a state equation linking the three quantities s, τ, a . Therefore, at equilibrium, the number of independent quantities is two, and one can write $v_m = f(G, a, \tau)$. Now, choosing as fundamental dimensional quantities the shear modulus G and the contact radius a , following Buckingham’s theorem [48–50] we write $v_m/a = g(\tau/G)$, and because of linear elasticity, we conclude that the functional form of $g(\tau/G)$ must be a relation of proportionality. Thus, the reduced displacement v_m/a is proportional to the reduced tangential stress τ/G , leading again to Eq. (8). In appendix A we present an analytical derivation of the interfacial tangential displacement field caused by uniform tangential tractions applied on a circular area of an elastic half-space, and demonstrate that $K = 2/\pi$. Therefore Eq. (8) becomes

$$v_m = \frac{2}{\pi G} \tau a = \frac{8}{\pi E^*} \tau a, \quad (9)$$

where we have introduced the reduced elastic modulus $E^* = E/(1 - \nu^2)$. It follows that $W = \pi a^2 v_m = 8\tau a^3/E^*$, and the energy term associated with the uniform stress distribution τ is then

$$\tau W = \frac{8\tau^2 a^3}{E^*}. \quad (10)$$

Notably, since $\nu = 0.5$, the normal displacement field is uncoupled from the tangential one. Thus, we can use the solution of the frictionless adhesive contact between a sphere and a half space. This solution is reported in [59], and it is easy to recover as the superposition of a rigid flat punch solution and Hertz solution. Therefore, the normal displacement field in the contact area is

$$u(\mathbf{x}) = s + \frac{|\mathbf{x}|^2}{2R},$$

and the normal stress field at the interface

$$\sigma(\mathbf{x}) = \sigma_0 \left(1 - \frac{|\mathbf{x}|^2}{a^2}\right)^{-1/2} + \sigma_1 \left(1 - \frac{|\mathbf{x}|^2}{a^2}\right)^{1/2}, \quad (11)$$

with

$$\sigma_0 = \frac{1}{\pi} E^* \left(\frac{s}{a} + \frac{a}{R}\right) \quad (12)$$

$$\sigma_1 = -\frac{1}{\pi} E^* \frac{2a}{R}. \quad (13)$$

As expected, when σ_0 is different from zero the stress distribution has a square root singularity as $|\mathbf{x}| \rightarrow a$. Negative values of σ_0 [*i.e.* $a < (-sR)^{1/2}$] are not physically acceptable since they would cause interpenetration of solids near the edges of the contact. Therefore only non-negative values of σ_0 are admissible, which is equivalent to say that the contact radius a must satisfy the following inequality

$$a \geq a_{Hz}, \quad (14)$$

where $a_{Hz} = (-sR)^{1/2}$ is the Hertzian contact radius that would be obtained in case of adhesiveless contacts at a given separation s . Moreover, for $a > a_{Hz}$ the interfacial tractive stress at the edge of the contact diverges towards infinitely large values. The latter scenario strictly requires tractive stresses to be developed in the contact, *i.e.* it can happen only in presence of adhesive forces. In absence of adhesion, instead, $\sigma_0 = 0$ and $a = a_{Hz}$.

A. Fixed separation

Now, given the separation s , we can calculate the thermodynamic potential $\mathcal{H}(s, \tau, a)$ from Eq. (5) as

$$\mathcal{H}(s, \tau, a) = E^* s^2 \left(a + \frac{2}{3} \frac{a^3}{R s} + \frac{1}{5} \frac{a^5}{R^2 s^2} \right) - \frac{4\tau^2 a^3}{E^*} - \pi \Delta \gamma a^2 \quad (15)$$

Notably, from Eq. (7) the normal force is

$$F = \left(\frac{\partial \mathcal{H}}{\partial s} \right)_{A, \tau} = E^* \left(2sa + \frac{2}{3} \frac{a^3}{R} \right). \quad (16)$$

In dimensionless terms, Eq. (15) becomes

$$\tilde{\mathcal{H}} = \tilde{a} - \frac{2}{3} \tilde{a}^3 + \frac{1}{5} \tilde{a}^5 - \tilde{\tau}^2 \tilde{a}^3 - \Delta \tilde{\gamma} \tilde{a}^2, \quad (17)$$

where we have defined the following reduced quantities:

$$\tilde{\mathcal{H}} = \frac{R^2 \mathcal{H}}{E^* a_{Hz}^5}; \quad \tilde{\tau} = \frac{2R\tau}{E^* a_{Hz}}; \quad \Delta \tilde{\gamma} = \pi \frac{R^2 \Delta \gamma}{E^* a_{Hz}^3}; \quad \tilde{a} = \frac{a}{a_{Hz}}. \quad (18)$$

Finally, enforcing Eq. (6) gives

$$\left(\frac{\partial \tilde{\mathcal{H}}}{\partial \tilde{a}} \right)_{\tilde{\tau}} = 1 - 2\tilde{a}^2 + \tilde{a}^4 - 3\tilde{\tau}^2 \tilde{a}^2 - 2\Delta \tilde{\gamma} \tilde{a} = 0, \quad (19)$$

which allows to determine the contact radius at equilibrium \tilde{a}_{eq} .

B. Fixed Load

In a similar way it is possible to address the contact case characterized by a constant normal force, F (configuration commonly adopted in experiments [34, 35, 38]). Again, we need to move to another thermodynamic potential \mathcal{G} by means of the new Legendre transformation

$$\mathcal{G} = \mathcal{H} - \left(\frac{\partial \mathcal{H}}{\partial s} \right)_{s, A} s = \mathcal{H} - F s. \quad (20)$$

Consequently, the equilibrium condition becomes

$$\left(\frac{\partial \mathcal{G}}{\partial A} \right)_{F, \tau} = 0. \quad (21)$$

Moreover, by using Eqs. (15, 16) we get

$$s = \frac{F}{2E^* a} - \frac{a^2}{3R}, \quad (22)$$

and

$$\mathcal{G}(F, \tau, a) = -\frac{F^2}{4E^* a} + \frac{F a^2}{3R} + \frac{4}{45} \frac{E^* a^5}{R^2} - \frac{4\tau^2 a^3}{E^*} - \pi \Delta \gamma a^2, \quad (23)$$

which in dimensionless form becomes

$$\tilde{\mathcal{G}} = \frac{R^2 \mathcal{G}}{E^* a_{Hz}^5} = -\frac{4}{9\tilde{a}} - \frac{4\tilde{a}^2}{9} + \frac{4\tilde{a}^5}{45} - \tilde{\tau}^2 \tilde{a}^3 - \Delta\tilde{\gamma} \tilde{a}^2, \quad (24)$$

where the definitions of $\tilde{\tau}$ and $\Delta\tilde{\gamma}$ are given in Eq. (18), and $a_{Hz} = -(3FR/4E^*)^{1/3}$.

Thus, from Eq. (21) we obtain

$$\frac{\partial \tilde{\mathcal{G}}}{\partial \tilde{a}} = \frac{4}{9\tilde{a}^2} - \frac{8\tilde{a}}{9} + \frac{4}{9}\tilde{a}^4 - 3\tilde{\tau}^2 \tilde{a}^2 - 2\Delta\tilde{\gamma} \tilde{a} = 0, \quad (25)$$

which allows to determine the equilibrium contact area at a given load.

III. RESULTS AND DISCUSSION

The above treatment makes it clear that the presence of the uniform tangential stresses at the interface acts as an additional (contact radius dependent) adhesive term. Indeed, both in Eqs. 15 and 23, an effective surface energy can be defined as

$$\Delta\gamma_{eff}(\tau, a) = \Delta\gamma + \frac{4\tau^2 a}{\pi E^*}. \quad (26)$$

Equation (26) shows that, given the tangential stress τ , the effective adhesion energy per unit area linearly increases with the contact radius a . Therefore, one concludes that in sliding contacts the term related to the tangential tractions should lead to an enhancement of the effective adhesion, and therefore to an increase of the contact area at equilibrium.

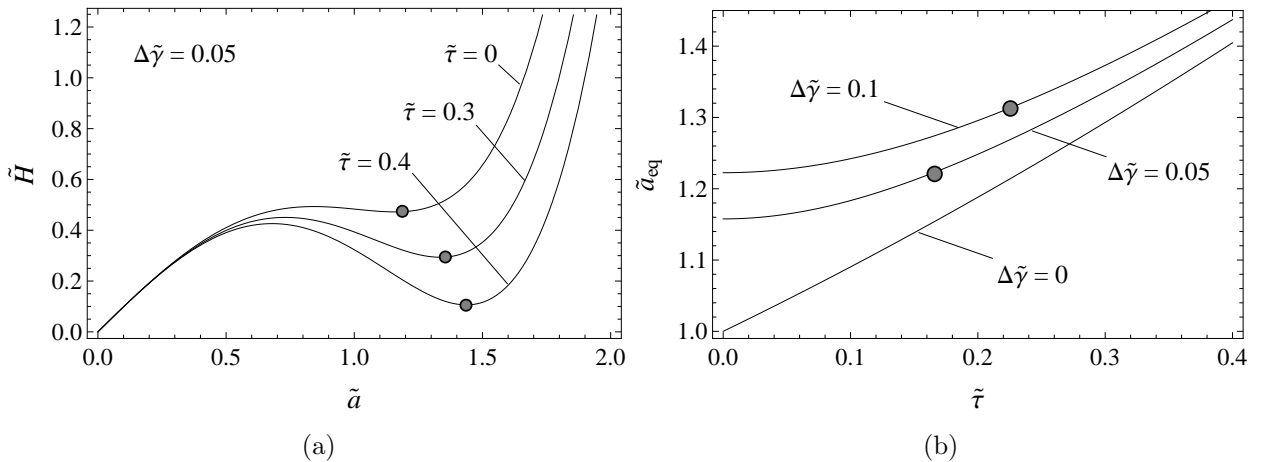


FIG. 2: Results diagrams under displacement controlled conditions: (a) The dimensionless energy as a function of the dimensionless contact area \tilde{a} . The circles represent stable equilibrium points. (b) The dimensionless equilibrium contact area as a function of the dimensionless shear stress $\tilde{\tau}$. The circles represent the threshold conditions beyond which significant influence of $\tilde{\tau}$ is predicted with respect to the corresponding frictionless case.

This is clearly shown in Fig. 2. In particular, Fig. 2a shows the dimensionless energy as a function of the contact area for different values of the dimensionless shear stress $\tilde{\tau}$. As

indicated by the circles, the stable equilibrium contact area increases with $\tilde{\tau}$. The same behavior is even clearer in Fig. 2b, where the dimensionless contact area at equilibrium is shown as a function of $\tilde{\tau}$. We observe that for very low values of $\tilde{\tau}$, the influence on the contact size with respect to the frictionless case is very weak. On the contrary, for large values of $\tilde{\tau}$, it becomes more and more significant. In order to estimate the threshold between these two conditions, we observe that, moving from Eqs. (19,25), a significant influence of $\tilde{\tau}$ is expected only for $3\tilde{\tau}^2\tilde{a}^2 > 2\Delta\tilde{\gamma}\tilde{a}$, i.e. for $\tilde{a} > 2\Delta\tilde{\gamma}/(3\tilde{\tau}^2)$. In Fig. 2b we reported the corresponding values by means of circles.

Moreover, from Fig. 2b, a contact area increase caused by interfacial shear stress (compared to the frictionless Hertzian value) is predicted even in the limiting case of $\Delta\gamma \rightarrow 0^+ > 0$. This result needs to be discussed as it seems to lead to a paradox since, a contact radius $a > a_{Hz}$ necessarily involves the presence of tractive stresses at the interface, which, in turn, cannot exist in the absence of adhesive forces. However, this paradox can be easily solved if one observes that, according to the Johnson Kendall and Roberts approach [41], adhesive interactions in our problem are described by extremely short range forces. In such a case the adhesive stresses are described in terms of a Dirac delta function

$$\sigma = -2\Delta\gamma\delta(r) = \lim_{\xi \rightarrow 0^+} -\frac{\Delta\gamma}{\xi} \exp\left(-\frac{r}{\xi}\right), \quad (27)$$

where ξ is the interaction characteristic length, and the limit is intended in a weak sense. It is then clear that for $r = 0$ we get $\sigma(0) = -\Delta\gamma/\xi$ which, even for extremely small but larger than zero values of $\Delta\gamma$ leads, to non zero extremely large forces as $\xi \rightarrow 0^+$.

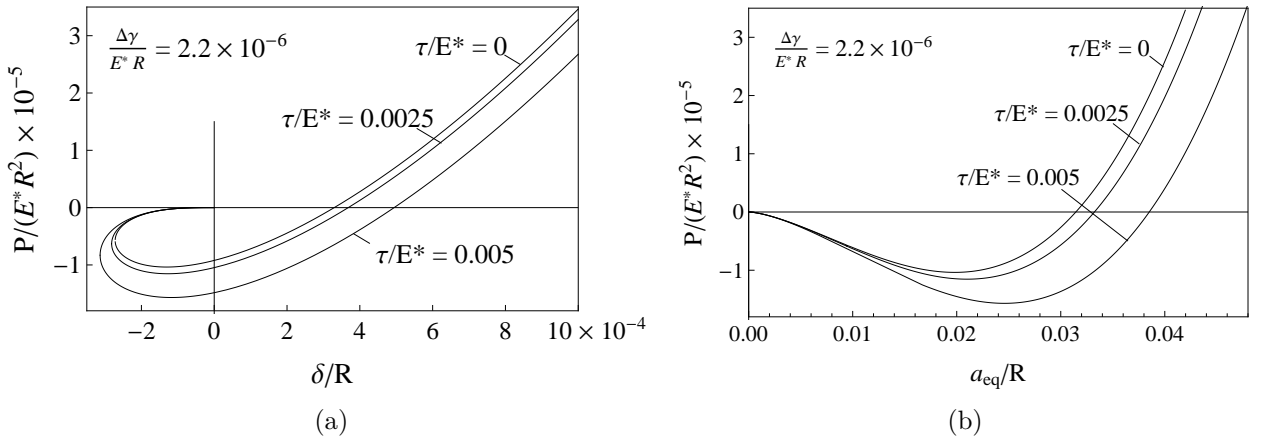


FIG. 3: Equilibrium diagrams of the dimensionless load as a function of: (a) the reduced penetration; (b) the reduced contact area.

Figures 3a and 3b show the dimensionless equilibrium compressive load $P/(E^*R^2)$, where $P = -F$, acting on the sphere as a function of the reduced contact penetration $\delta/R = -s/R$ and contact size a/R , respectively. Interestingly, the effect of interfacial shear stresses is to reduce the equilibrium load at any given value of δ or a . This peculiarity, and in particular the enhancement of the pull-off force, is more clearly shown by Fig. 4, where the dimensionless pull-off load is plotted against τ/E^* . Interestingly, enhanced adhesive strength is predicted when tangential tractions affect the contact. A similar mechanism, as already suggested in Ref. [52], may be at the origin of the observed gecko ability to

control the adhesive behavior by shearing oppositely the toes adhering to the substrate, which cannot be predicted for example using Kendall's peeling theory.

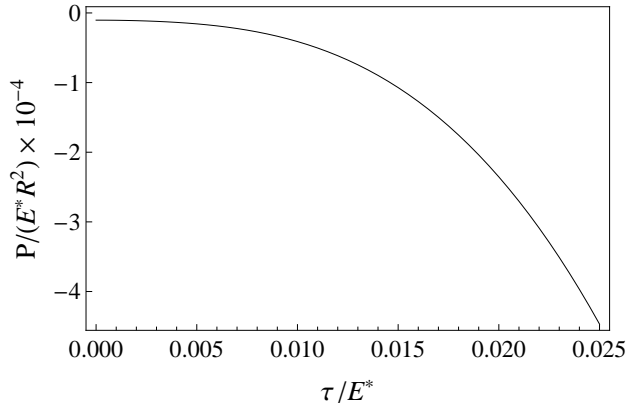


FIG. 4: The dimensionless pull-off load as a function of the reduced shear stress.

Fig. 5 shows the comparison between load and displacement controlled equilibrium contact area: the increase of the contact area, for any given value of $\tilde{\tau} > 0$, is larger for the load controlled case compared to displacement controlled conditions.

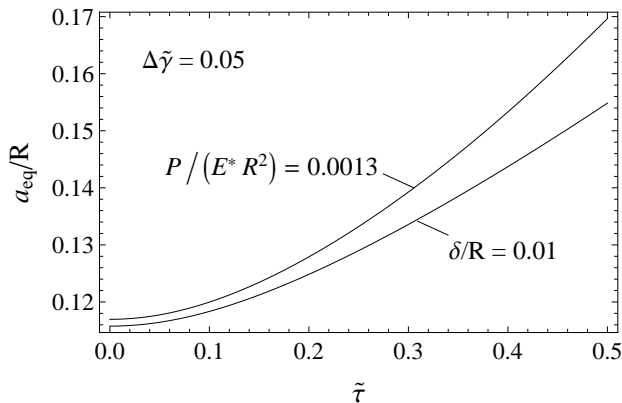


FIG. 5: Comparison between equilibrium dimensionless contact area \tilde{a} as a function of dimensionless shear stress $\tilde{\tau}$ for load and displacement controlled conditions. Notably, the values assumed for P and δ corresponds to $a_{Hz}/R = 0.1$.

The above arguments seems to disprove the fact that sliding friction hinders adhesion, thus contravening what is commonly accepted in the scientific literature. So the question is: are we wrong or something new can be drawn from these results? To answer this question we need to revisit some of the most interesting experiments on the topic. Several of them [35, 36, 38] show that adhesion totally disappears for sufficiently high sliding velocity. Among them, we identify the work by Vorvolakos and Chaudhury [35] as one of the most interesting in the field. Focusing on Fig. 7 of the cited paper [35], we note that the contact area reduction is observed only for sliding velocities larger than 2-3 mm/s, and the resulting contact area is even smaller than the Hertzian predicted value. With respect to this peculiar behavior, most of the existing literature refers to the seminal paper by Savkoor and Briggs [34], where the authors justify the contact area reduction relying on fracture mechanics arguments.

Specifically, they assume uniform tangential displacement at the interface (i.e. they are controlling the tangential displacement rather than the tangential frictional tractions), which gives rise to a shear stress singularity at the contact area edges which, in turn, is modelled as a mode II crack opening. Eventually, the Griffith equilibrium condition predict a reduction of the contact area size. However, from a theoretical point of view, we observe that the main assumption behind this result is that the displacement distribution over the contact area is uniform. This physical picture clearly refers to the case of a fully stuck contact under externally applied tangential load. On the contrary, when gross sliding is developed between the two interfaces, frictional shear stresses are prescribed instead of continuity of displacements across the interface. As shown in several previous work e.g. [46, 47], in the case of soft polymers shear stresses are distributed more or less uniformly (apart from fluctuations, also covered in this study) over the sliding contact area. We therefore conclude that since under gross slip there is no shear stress singularity in the contact, the model proposed by Savkoor and Briggs is not able to capture the physics of sliding adhesive contacts in full. Very interestingly, to the best of authors knowledge there are two studies [39, 40] which clearly support this conclusion, as they both measure an increase of the contact area at moderate sliding velocities. In particular in Ref. [39] an increase of contact area not less than 12 – 18% is measured at sliding velocity up to 12mm/s, whereas, for larger velocities, a fast decrease is then observed. In Ref. [40] the sliding contact of a soft sphere against a rough much stiffer substrate is measured for sliding velocity ranging from 20 – 50 μ m/s. Also in this case an increase of contact area from 13 – 23% is observed. Moreover, Refs [35, 36] clearly show that a significant reduction of the contact area only happens at sufficiently high sliding velocity, and for soft solids always associate with the transition toward a stick-slip regime. In particular some experiments [35, 36, 38] show that, at low sliding velocity, although gross slip condition are already established, no contact area reduction is observed. It is, then, evident that this behavior cannot be explained by relying on the Savkoor and Briggs model. Therefore, the contact area reduction observed in Refs [36, 38] as well as in Fig. 7 in Ref. [35] must have a different origin. To this regard we believe that some coexisting mechanisms can be identified as the root cause of the contact area reduction (i) the reduction of adhesive bonds at the interface, (ii) the large non-linear interfacial deformations, and (iii) the shear stress fluctuations at the interface. The first relies on the reduction of the adhesive bonds induced by the relative motion between the contacting surfaces. Indeed, as pointed out firstly by Schallamach [42] and then by many other authors [35, 36, 53, 54], this relative motion leads to an increase of the debonding ratio, whereas the rebinding ratio remains almost constant. The balance between these ratios can, for sufficiently high sliding velocity, almost completely mask adhesion. The second mechanism, causing the observed drop of the contact area below the Hertz theory prediction, must be ascribed to non-linear large deformations caused by the tangential tractions at the interface, as indeed reported in similar range of velocities in Refs. [36, 46, 55]. The third mechanism, discussed in Sec. IV, is related to the genesis of a surface repulsive energy term associated with the random fluctuations of the shear stresses at the interface, which is expected to become very significant at the onset of the stick-slip motion.

It is worth noting that, since the second mechanism is shear dependent, at very low sliding velocity it can be mitigated by the reduction in shear stresses at the interface (see Refs [35, 46]). However, the first mechanism still takes place at very low sliding velocities, as indeed shown in Ref [53] where a reduction of 15-20% of the number of adhesive bonds is predicted at sliding velocity well below the stick-slip transition. Moreover, referring to Ref [42], the

adhesive bonds number can be estimated as $N = N_0 / (1 + V/V_c)$, where N_0 are the number of bonds at rest, and V_c is the critical speed. In the case of PDMS (Polydimethylsiloxane) adhesive behavior, the latter has been estimated as $V_c \approx 1\text{-}5$ mm/s in both Refs [35, 36].

According to the Schallamach equation, we observe that $N \approx 0.9N_0$ already at $V \approx 0.1$ mm/s, and it reduces down to $N \approx 0.5N_0$ at $V \approx 1$ mm/s. We would therefore expect to observe a significant reduction of the contact area already at velocities in the range 0.1-1 mm/s, not observed in Ref. [35]. We believe that this interesting result can be explained by our model by observing that, in the prescribed range of sliding velocity (0.1-1mm/s), the energy contribution due to tangential force (see Eqs. (15,23)) favors adhesion, therefore balancing the reduction of $\Delta\gamma$ and leaving the contact area unaltered as indeed shown in Fig. 7 of Ref. [35]. On the contrary, a significant reduction of the contact area compared to the JKR predictions is observed only for $V > 2\text{-}3$ mm/s (see Fig. 7 in Ref. [35]) when the contact moves from a stable sliding to the stick-slip regime. In such a case as shown in Sec. IV the strong shear stress fluctuations produce a repulsive surface energy term that hinders the interfacial adhesion.

IV. THE EFFECT OF TANGENTIAL STRESS FLUCTUATIONS

So far we have considered the case where the tangential frictional stress is uniformly distributed at the interface. However, fluctuations in the stress field may be present, which, as we show below, may have a non-negligible effect on the contact. In this section we look specifically at this point. So assume that the tangential frictional stress field at the interface is given by the sum of an average stress τ_0 and a fluctuating term $\tau_1(\mathbf{x})$, i.e.

$$\tau(\mathbf{x}) = \tau_0 + \tau_1(\mathbf{x}) \quad (28)$$

where the ensemble average $\langle \tau_1(\mathbf{x}) \rangle = 0$. The symbol $\langle \cdot \rangle$ is used in the sequel to represent the ensemble average operator. Assuming that the contact area is sufficiently large compared to the wavelengths of the fluctuating stress field $\tau_1(\mathbf{x})$, local ergodicity allows us to replace the spatial averages with the ensemble averages. Now observe that, because of linear elasticity, we can also write the tangential displacement field $v(\mathbf{x})$ as the sum of two terms

$$v(\mathbf{x}) = w_0(\mathbf{x}) + w_1(\mathbf{x}) \quad (29)$$

where

$$w_0(\mathbf{x}) = \int d^2x' G_x(\mathbf{x} - \mathbf{x}') \tau_0 \quad (30)$$

$$w_1(\mathbf{x}) = \int d^2x' G_x(\mathbf{x} - \mathbf{x}') \tau_1(\mathbf{x}') \quad (31)$$

where the Green function $G_x(\mathbf{x})$ is given in Eq. (A1). Since $\langle w_1(\mathbf{x}) \rangle = 0$, we get $W = \int d^2x v(\mathbf{x}) = \int d^2x w_0(\mathbf{x})$. So, the elastic energy of the system becomes

$$\mathcal{E} = \frac{1}{2} \int_{\Omega} d^2x \sigma(\mathbf{x}) u(\mathbf{x}) + \frac{1}{2} \tau_0 W + \frac{1}{2} \int_{\Omega} d^2x \tau_1(\mathbf{x}) v(\mathbf{x}) \quad (32)$$

Now note that $\langle \tau_1(\mathbf{x}) v(\mathbf{x}) \rangle = \langle \tau_1(\mathbf{x}) w_1(\mathbf{x}) \rangle$, thus Eq. (32) can be rephrased as

$$\mathcal{E} = \frac{1}{2} \int_{\Omega} d^2x \sigma(\mathbf{x}) u(\mathbf{x}) + \frac{1}{2} \tau_0 W + \frac{1}{2} \langle \tau_1(\mathbf{x}) w_1(\mathbf{x}) \rangle A \quad (33)$$

where because of ergodicity the quantity $\frac{1}{2} \langle \tau_1(\mathbf{x}) w_1(\mathbf{x}) \rangle = \Delta\Gamma$ is independent of the position vector \mathbf{x} and represents a surface energy per unit area. Using Eq. (31) this surface energy $\Delta\Gamma$ can be easily calculated as

$$\langle \tau_1(\mathbf{x}) w_1(\mathbf{x}) \rangle = \int d^2x' G_x(\mathbf{x} - \mathbf{x}') \langle \tau_1(\mathbf{x}) \tau_1(\mathbf{x}') \rangle = \int d^2x G_x(\mathbf{x}) \langle \tau_1(\mathbf{x}) \tau_1(\mathbf{0}) \rangle \quad (34)$$

Eq. (34) has also an analogous expression in Fourier space which may be easier to calculate. Note that by taking the Fourier transform of Eq. (A1) we get

$$G_x(\mathbf{q}) = \int d^2x G_x(\mathbf{x}) e^{-i\mathbf{q}\cdot\mathbf{x}} = \frac{1}{2G} \frac{1}{q} \left(1 + \frac{q_y^2}{q^2} \right) \quad (35)$$

then taking the Fourier transform of Eq. (31) we also obtain

$$w_1(\mathbf{q}) = G_x(\mathbf{q}) \tau_1(\mathbf{q}). \quad (36)$$

Using

$$\langle \tau_1(\mathbf{x}) w_1(\mathbf{x}) \rangle = \frac{1}{(2\pi)^4} \int d^2q d^2q' \langle \tau_1(\mathbf{q}) w_1(\mathbf{q}') \rangle e^{i\mathbf{q}\cdot\mathbf{x}} e^{i\mathbf{q}'\cdot\mathbf{x}} \quad (37)$$

and replacing Eq. (36) in Eq. (37) we get

$$\langle \tau_1(\mathbf{x}) w_1(\mathbf{x}) \rangle = \frac{1}{(2\pi)^4} \int d^2q d^2q' G_x(\mathbf{q}') \langle \tau_1(\mathbf{q}) \tau_1(\mathbf{q}') \rangle e^{i\mathbf{q}\cdot\mathbf{x}} e^{i\mathbf{q}'\cdot\mathbf{x}} \quad (38)$$

The quantity $\langle \tau_1(\mathbf{q}) \tau_1(\mathbf{q}') \rangle = (2\pi)^2 C_\tau(\mathbf{q}) \delta(\mathbf{q} + \mathbf{q}')$, where the power spectral density of the stress fluctuation at the interface is $C_\tau(\mathbf{q}) = \int d^2x \langle \tau(\mathbf{x}) \tau(\mathbf{0}) \rangle e^{-i\mathbf{q}\cdot\mathbf{x}}$. Therefore we obtain

$$\langle \tau_1(\mathbf{x}) w_1(\mathbf{x}) \rangle = \int d^2x G_x(\mathbf{x}) \langle \tau(\mathbf{x}) \tau(\mathbf{0}) \rangle = \frac{1}{(2\pi)^2} \int d^2q G_x(\mathbf{q}) C_\tau(\mathbf{q}) \quad (39)$$

which allows us to calculate the surface energy per unit area $\Delta\Gamma$ as

$$\Delta\Gamma = \frac{1}{8\pi^2} \int d^2q G_x(\mathbf{q}) C_\tau(\mathbf{q}) > 0 \quad (40)$$

and the elastic energy

$$\mathcal{E} = \frac{1}{2} \int_{\Omega} d^2x \sigma(\mathbf{x}) u(\mathbf{x}) + \frac{1}{2} \tau_0 W + \Delta\Gamma A = \mathcal{E}_0 + \Delta\Gamma A. \quad (41)$$

The total energy of the system is then

$$\mathcal{U}(s, W, A) = \mathcal{E}_0(s, W, A) - (\Delta\gamma - \Delta\Gamma) A. \quad (42)$$

Equation (42) shows that the effect of tangential stress fluctuation $\tau_1(\mathbf{x})$ at the interface consists in including a ‘repulsive’ surface energy term per unit area, which diminishes the adhesion energy $\Delta\gamma$ per unit area of the amount $\Delta\Gamma$. Thus, by replacing $\Delta\gamma \rightarrow \Delta\gamma - \Delta\Gamma$ the original formulation of Sec. II, is easily retrieved. Note that if the fluctuations of the interfacial tangential stresses are sufficiently large [i.e. significant values of $C_\tau(\mathbf{q})$] the term $\Delta\Gamma$ may become comparable with $\Delta\gamma$ and, in the end, may even counterbalance or overcome

the effect of the uniform stress at the interface, thus leading to a reduction of the contact area. Indeed, such fluctuations are strongly enhanced at the onset of stick-slip motion. This may explain why above a certain velocity threshold, $V > 2\text{-}3$ mm/s, a strong reduction of contact area is observed, as shown in Ref. [35].

To estimate the amplitude of shear stress fluctuations necessary to completely mask the adhesion energy, let us now consider the simple case of a sinusoidal fluctuation of the shear stress field, i.e. let us assume that $\tau_1(\mathbf{x}) = \tau_1 \cos(q_k x + \varphi) = \frac{1}{2}\tau_1 [\exp(iq_k x) \exp(i\varphi) + \exp(-iq_k x) \exp(-i\varphi)]$, where $0 \leq \varphi < 2\pi$ is a uniformly distributed random phase. Then we obtain

$$\langle \tau(\mathbf{x}) \tau(\mathbf{0}) \rangle = \frac{1}{4}\tau_1^2 (e^{iq_k x} + e^{-iq_k x}) = \frac{1}{2}\tau_1^2 \cos(q_k x) \quad (43)$$

Taking the Fourier transform we obtain

$$C_\tau(\mathbf{q}) = \int d^2x \langle \tau(\mathbf{x}) \tau(\mathbf{0}) \rangle e^{-i\mathbf{q}\cdot\mathbf{x}} = \pi^2 \tau_1^2 \delta(q_y) \{ \delta(q_x - q_k) + \delta(q_x + q_k) \} \quad (44)$$

substituting Eq. (44) into Eq. (40) we get

$$\Delta\Gamma = \frac{\tau_1^2}{8G} \frac{1}{q_k} = \frac{\tau_1^2}{16\pi G} \lambda_k = \frac{\tau_1^2}{16\pi G} \frac{L}{k} \quad (45)$$

where $L \approx 2a$ is the lateral size of the contact area. Therefore the amplitude τ_1 of the fluctuating stress needed to fully cancel the effect of adhesion, i.e. to make $\Delta\Gamma = \Delta\gamma$ is

$$\tau_1 = 4\sqrt{\pi k \frac{G\Delta\gamma}{L}}.$$

Assuming $k = 10$, and as in Ref. [35], $G = 1.6\text{MPa}$, $L = 0.24\text{mm}$, $\Delta\gamma = 42\text{mJ/m}^2$ we get $\tau_1 \approx 375\text{kPa}$. Using the data from Ref. [46], i.e. $G = 0.5\text{MPa}$, $L = 4\text{mm}$, and $\Delta\gamma = 42\text{mJ/m}^2$ we get $\tau_1 \approx 51\text{kPa}$. Therefore, the intensity of shear stress fluctuations needed to completely mask adhesion is as large as the average stress τ_0 at the interface. Such large fluctuation may occur in the contact area of soft-solids at the one-set of stick-slip. Should these stress-fluctuation really be observed under stick-slip conditions, they would provide an additional important step toward the complete understanding of the physics governing the reduction of the size of the contact area in sliding contacts. This emphasizes the need for further experimental investigations in which fluctuations, as well as contact area and frictional force, are captured to shed light on the complex interplay between adhesion and tangential interfacial stresses.

V. CONCLUSIONS

In this work we have investigated the effect of interfacial tangential tractions on the contact area evolution in adhesive sliding contacts, under gross slip conditions. We developed a theoretical model which, relying on energetic arguments, takes into account the mechanical energy term related to the applied tangential tractions, regardless of their nature and cause (frictional, chemical, etc.). We focused on the exemplar case of a rigid smooth sphere in sliding contact with an elastic half-space. The model shows that an increase of the

contact area with respect to the static adhesive condition (namely the JKR case) should be observed due to the uniform shear stress occurring at the interface. In fact, this uniform stress produces an attractive surface energy term, which acts as an adhesion ‘booster’. This is specifically true at low velocity before the onset of stick-slip. In fact at low-speed sliding, the shear stress fluctuations at the interface, which produce an apparent repulsive surface energy term, are negligible compared to the average stress. When the contact moves into the stick-slip regime the shear stress fluctuations may become comparable to the average interfacial stress leading to a strong repulsive surface energy. This may explain why adhesion is completely masked at relatively large sliding velocities. This scenario seems to be, at least partially, confirmed in the scientific experimental literature.

Acknowledgement 1 *The authors thanks Bo Persson and Antoine Chateaubinois for valuable scientific discussions, as well as the referees for the interesting suggestions. D.D. would like to acknowledge the support received from the Engineering and Physical Sciences Research Council (EPSRC) via his Established Career Fellowship EP/N025954/1.*

APPENDIX A: THE ELASTIC TANGENTIAL DISPLACEMENT FIELD OVER A CIRCULAR REGION LOADED WITH UNIFORMLY DISTRIBUTED TANGENTIAL STRESSES.

In this section we calculate the tangential displacement field due to uniform and uni-directional tangential traction acting along the x axis on an elastic half-space surface and distributed over circular area of radius a . We focus, for simplicity, on incompressible materials (so that there is no interaction between normal and tangential fields) with Poisson’s ratio $\nu = 0.5$. In such a case, we recall that the surface tangential displacement $G_x(\mathbf{x})$ due to a concentrated unit force $F_x = 1$ placed at the origin of the half-space and tangentially directed along the x axis is (see Refs [56, 57])

$$G_x(\mathbf{x}) = \frac{1 + \nu}{2\pi E} \frac{1}{|\mathbf{x}|} \left[2(1 - \nu) + 2\nu \frac{x^2}{|\mathbf{x}|^2} \right] = \frac{3}{4\pi E} \frac{1}{|\mathbf{x}|} \left(1 + \frac{x^2}{|\mathbf{x}|^2} \right) = \frac{1}{4\pi G} \frac{1}{|\mathbf{x}|} + \frac{1}{4\pi G} \frac{x^2}{|\mathbf{x}|^3} \quad (\text{A1})$$

where G is the shear modulus.

The surface tangential displacement due to a uniform tangential stress $\tau_x(\mathbf{x}) = \tau_0$ acting on a circular area can be found as the convolution integral on the contact area of Eq. A1

$$v(\mathbf{x}) = \frac{\tau_0}{4\pi G} \int d^2x' \frac{1}{|\mathbf{x} - \mathbf{x}'|} + \frac{\tau_0}{4\pi G} \int d^2x' \frac{(x - x')^2}{|\mathbf{x} - \mathbf{x}'|^3} = v_1(\mathbf{x}) + v_2(\mathbf{x}) \quad (\text{A2})$$

The first term in Eq. (A2) is the analogues of the normal displacement at the interface obtained with the application of a uniform pressure distribution on a circular area of radius a . The solution is given by Johnson. In such a case we get that within the loaded circle

$$v_1(\mathbf{x}) = \frac{\tau_0}{4\pi G} \int d^2x' \frac{1}{|\mathbf{x} - \mathbf{x}'|} = \frac{\tau_0 a}{\pi G} E(\rho); \quad \rho < 1 \quad (\text{A3})$$

where $\rho = r/a$, and $E(\rho) = \int_0^{\pi/2} \sqrt{1 - \rho^2 \sin^2 \varphi} d\varphi$ is the elliptic integral of the second kind.

Furthermore, by defining $\mathbf{s} = \mathbf{x} - \mathbf{x}'$ and

$$x' - x = s \cos \varphi \quad (\text{A4})$$

$$y' - y = s \sin \varphi \quad (\text{A5})$$

the second term in Eq. (A2) can be rewritten as

$$v_2(\mathbf{x}) = \frac{\tau_0}{4\pi G} \int_0^{2\pi} d\varphi \cos^2 \varphi \int_0^{s_1} ds = \frac{\tau_0}{4\pi G} \int_0^{2\pi} d\varphi \sqrt{a^2 - r^2 \sin^2(\varphi - \theta)} \cos^2 \varphi \quad (\text{A6})$$

where $s_1(\varphi) = -x \cos \varphi - y \sin \varphi + \sqrt{a^2 - (x \sin \varphi - y \cos \varphi)^2}$, $x = r \cos \theta$, and $y = r \sin \theta$.

Finally, after a few algebraic manipulations Eq. (A6) gives

$$v_2(\mathbf{x}) = \frac{\tau_0 a}{2\pi G} \left[1 + \frac{1}{3} \frac{2 - \rho^2}{\rho^2} \cos(2\theta) \right] E(\rho) - \frac{1}{3} \frac{\tau_0 a}{\pi G} \frac{1 - \rho^2}{\rho^2} \cos(2\theta) K(\rho); \quad \rho < 1 \quad (\text{A7})$$

where $K(\rho) = \int_0^{\pi/2} d\varphi (1 - \rho^2 \sin^2 \varphi)^{-1/2}$ is complete Elliptic integral of first kind

Therefore, combining Eqs. (A3,A7) with Eq. (A2), the tangential displacement field due to uniform and unidirectional tangential tractions over a circular contact is

$$\begin{aligned} v(\mathbf{x}) &= v_1(\mathbf{x}) + v_2(\mathbf{x}) \\ &= \frac{3}{2} \frac{\tau_0 a}{\pi G} E(\rho) + \frac{1}{3} \frac{\tau_0 a}{2\pi G} \frac{2 - \rho^2}{\rho^2} E(\rho) \cos(2\theta) - \frac{1}{3} \frac{\tau_0 a}{\pi G} \frac{1 - \rho^2}{\rho^2} K(\rho) \cos(2\theta); \quad \rho < 1 \end{aligned} \quad (\text{A8})$$

Notably, the mean displacement v_m in the contact area is

$$v_m = \frac{1}{\pi a^2} \int v(\mathbf{x}) d^2x = \frac{1}{\pi a^2} \int dr d\theta r v(r, \theta) = \frac{2\tau_0 a}{\pi G} \quad (\text{A9})$$

-
- [1] Hunter S.C. , The rolling contact of a rigid cylinder with a viscoelastic half space Trans. ASME, Ser. E, J. Appl. Mech. 28, 611–617, 1961.
 - [2] Grosch K. A. , The Relation between the Friction and Visco-Elastic Properties of Rubber, Proceedings of the Royal Society of London. Series A, Mathematical and Physical, 274-1356, 21-39, 1963.
 - [3] Panek C. and Kalker J.J., Three-dimensional Contact of a Rigid Roller Traversing a Viscoelastic Half Space, J. Inst. Maths Applies 26, 299-313, 1980.
 - [4] Persson B.N.J., Theory of rubber friction and contact mechanics, Journal of Chemical Physics, 115, 3840 -3861, 2001.
 - [5] Persson B.N.J., Rolling friction for hard cylinder and sphere on viscoelastic solid, Eur. Phys. J. E, 33, 327-333, 2010.
 - [6] M. Harrass, K.Friedrich , A.A.Almajid, Tribological behavior of selected engineering polymers under rolling contact, Tribology International, 43, 635–646, 2010.

- [7] Menga N, Putignano C, Carbone G, Demelio GP. 2014 The sliding contact of a rigid wavy surface with a viscoelastic half-space. *Proc. R. Soc. A*, 470, 20140392, 2014.
- [8] Padovan J., O. Paramadilok, Transient and steady state viscoelastic rolling contact, *Comput Struct*, 20, 545-553, 1984.
- [9] Padovan J., Finite element analysis of steady and transiently moving/rolling nonlinear viscoelastic structure-I. theory. *Computers & Structures*, 27(2):249–257, 1987.
- [10] Padovan J., Kazempour A., Tabaddor F. and Brockman B., Alternative formulations of rolling contact problems. *Finite Elements in Analysis and Design*, 11:275–284, 1992.
- [11] L. Nasdala, M. Kaliske, A. Becker, H. Rothert, An efficient viscoelastic formulation for steady-state rolling structures, *Computational Mechanics* 22, 395-403, 1998.
- [12] Le Tallec P., Rahler C., Numerical models of steady rolling for non-linear viscoelastic structures in finite deformations, *International Journal for Numerical Methods in Engineering*, 37, 1159-1186, 1994.
- [13] Menga, N., Afferrante, L., & Carbone, G. (2016). Effect of thickness and boundary conditions on the behavior of viscoelastic layers in sliding contact with wavy profiles. *Journal of the Mechanics and Physics of Solids*, 95, 517-529.
- [14] Menga, N., Afferrante, L., & Carbone, G. (2016). Adhesive and adhesiveless contact mechanics of elastic layers on slightly wavy rigid substrates. *International Journal of Solids and Structures*, 88, 101-109.
- [15] Menga, N., Foti, D., & Carbone, G. Viscoelastic frictional properties of rubber-layer roller bearings (RLRB) seismic isolators. *Meccanica*, 1-11.
- [16] Schapery R.A., On the characterization of nonlinear viscoelastic materials, *Polymer Engineering & Science*, 9(4), 295-310, 1969.
- [17] Faisca R.G, Magluta C. and Roitman N., Experimental Characterization of Viscoelastic Materials as Vibration Dampers, *Journal of Engineering Mechanics*, 127(9), 959-962, 2001.
- [18] Odegard G.M., Gates T.S. and Herring H.M., Characterization of viscoelastic properties of polymeric materials through nanoindentation, *Experimental Mechanics*, 45(2), 130-136, 2005.
- [19] Carbone G., Lorenz B., Persson B.N.J. and Wohlers A., Contact mechanics and rubber friction for randomly rough surfaces with anisotropic statistical properties, *The European Physical Journal E – Soft Matter*, 29(3), 275–284, 2009.
- [20] Martina D., Creton C., Damman P., Jeusette M. and Lindner A., Adhesion of soft viscoelastic adhesives on periodic rough surfaces, *Soft Matter* 8(19), 5350-5357, 2012.
- [21] Theodore, A. N., Samus, M. A., & Killgoar Jr, P. C. (1992). Environmentally durable elastomer materials for windshield wiper blades. *Industrial & engineering chemistry research*, 31(12), 2759-2764.
- [22] Dimaki, A. V., Dmitriev, A. I., Menga, N., Papangelo, A., Ciavarella, M., Popov, V. L. Fast High-Resolution Simulation of the Gross Slip Wear of Axially Symmetric Contacts. *Tribology Transactions* 59-1 (2016): 189-194.
- [23] Menga, Nicola, and Michele Ciavarella. "A Winkler solution for the axisymmetric Hertzian contact problem with wear and finite element method comparison." *The Journal of Strain Analysis for Engineering Design* 50.3 (2015): 156-162.
- [24] Extrand, C. W., Gent, A. N., & Kaang, S. Y. (1991). Friction of a rubber wedge sliding on glass. *Rubber chemistry and technology*, 64(1), 108-117.
- [25] Newby, B. M. Z., Chaudhury, M. K., & Brown, H. R. (1995). Macroscopic evidence of the effect of interfacial slippage on adhesion. *Science*, 269(5229), 1407.
- [26] Zhang Newby, B. M., & Chaudhury, M. K. (1998). Friction in adhesion. *Langmuir*, 14(17),

4865-4872.

- [27] Persson, B. N. J., Albohr, O., Tartaglino, U., Volokitin, A. I., & Tosatti, E. (2004). On the nature of surface roughness with application to contact mechanics, sealing, rubber friction and adhesion. *Journal of Physics: Condensed Matter*, 17(1), R1.
- [28] Pohl, A., Steindl, R., & Reindl, L. (1999). The "intelligent tire" utilizing passive SAW sensors measurement of tire friction. *IEEE transactions on instrumentation and measurement*, 48(6), 1041-1046.
- [29] Nusbaum, H. J., Rose, R. M., Paul, I. L., Crugnola, A. M., & Radin, E. L. (1979). Wear mechanisms for ultrahigh molecular weight polyethylene in the total hip prosthesis. *Journal of Applied Polymer Science*, 23(3), 777-789.
- [30] Dong, H., Bell, T., Blawert, C., & Mordike, B. L. (2000). Plasma immersion ion implantation of UHMWPE. *Journal of materials science letters*, 19(13), 1147-1149.
- [31] Yi, F., Zhang, M., & Xu, Y. (2005). Effect of the electric current on the friction and wear properties of the CNT-Ag-G composites. *Carbon*, 43(13), 2685-2692.
- [32] Adams, J. B., Hector, L. G., Siegel, D. J., Yu, H., & Zhong, J. (2001). Adhesion, lubrication and wear on the atomic scale. *Surface and interface analysis*, 31(7), 619-626.
- [33] Stanley, H. M., Etsion, I., & Bogoy, D. B. (1990). Adhesion of contacting rough surfaces in the presence of sub-boundary lubrication. *ASME J. Tribol*, 112(1), 98-104.
- [34] Savkoor, A. R., & Briggs, G. A. D. (1977, August). The effect of tangential force on the contact of elastic solids in adhesion. In *Proceedings of the Royal Society of London A: Mathematical, Physical and Engineering Sciences* (Vol. 356, No. 1684, pp. 103-114). The Royal Society.
- [35] Vorvolakos, K., & Chaudhury, M. K. (2003). The effects of molecular weight and temperature on the kinetic friction of silicone rubbers. *Langmuir*, 19(17), 6778-6787.
- [36] Wu-Bavouzet, F., Clain-Burckbuchler, J., Buguin, A., De Gennes, P. G., & Brochard-Wyart, F. (2007). Stick-slip: Wet versus dry. *The Journal of Adhesion*, 83(8), 761-784.
- [37] Johnson, K. L. (1997). Adhesion and friction between a smooth elastic spherical asperity and a plane surface. In *Proceedings of the Royal Society of London A: Mathematical, Physical and Engineering Sciences* (Vol. 453, No. 1956, pp. 163-179). The Royal Society.
- [38] Homola, A. M., Israelachvili, J. N., McGuiggan, P. M., & Gee, M. L. (1990). Fundamental experimental studies in tribology: the transition from "interfacial" friction of undamaged molecularly smooth surfaces to "normal" friction with wear. *Wear*, 136(1), 65-83.
- [39] Arvanitaki, A., Briscoe, B. J., Adams, M. J., & Johnson, S. A. (1995). The friction and lubrication of elastomers. *Tribology Series*, 30, 503-511.
- [40] Krick, B. A., Vail, J. R., Persson, B. N., & Sawyer, W. G. (2012). Optical in situ micro tribometer for analysis of real contact area for contact mechanics, adhesion, and sliding experiments. *Tribology Letters*, 45(1), 185-194.
- [41] Johnson, K. L., Kendall, K., & Roberts, A. D. (1971, September). Surface energy and the contact of elastic solids. In *Proceedings of the Royal Society of London A: Mathematical, Physical and Engineering Sciences* (Vol. 324, No. 1558, pp. 301-313). The Royal Society.
- [42] Schallamach, A. (1963). A theory of dynamic rubber friction. *Wear*, 6(5), 375-382.
- [43] Chernyak, Y. B., & Leonov, A. I. (1986). On the theory of the adhesive friction of elastomers. *Wear*, 108(2), 105-138.
- [44] Persson B N J , Sivebaek I.M. , Samoilov V. N., Zhao Khe, Volokitin A.I., Zhang Zhenyu, (2008). On the origin of Amonton's friction law, *J. Phys.: Condens. Matter* **20** 395006.
- [45] Gao, J., Luedtke, W. D., Gourdon, D., Ruths, M., Israelachvili, J. N., & Landman, U. (2004). Frictional forces and Amontons' law: from the molecular to the macroscopic scale.

- [46] Chateauminois, A., & Fretigny, C. (2008). Local friction at a sliding interface between an elastomer and a rigid spherical probe. *The European Physical Journal E: Soft Matter and Biological Physics*, 27(2), 221-227.
- [47] Scheibert J., Prevost A., Frelat J., Rey P., Debrégeas G., (2008). Experimental evidence of non-Amontons behaviour at a multi-contact interface, *EPL* **83** 34003
- [48] Buckingham, E. (1914). On physically similar systems; illustrations of the use of dimensional equations. *Physical review*, 4(4), 345.
- [49] Buckingham, E. (1915). The principle of similitude. *Nature*, 96(2406), 396-397.
- [50] Buckingham E., Model experiments and the form of empirical equations, *Trans. ASME* 37 (1915) 263.
- [51] Gibbs, J. W. (1878). On the equilibrium of heterogeneous substances. *American Journal of Science*, (96), 441-458.
- [52] Autumn, K., Dittmore, A., Santos, D., Spenko, M., & Cutkosky, M. (2006). Frictional adhesion: a new angle on gecko attachment. *Journal of Experimental Biology*, 209(18), 3569-3579.
- [53] Filippov, A. E., Klafter, J., & Urbakh, M. (2004). Friction through dynamical formation and rupture of molecular bonds. *Physical Review Letters*, 92(13), 135503.
- [54] Gravish, N., Wilkinson, M., Sponberg, S., Parness, A., Esparza, N., Soto, D., ... & Autumn, K. (2010). Rate-dependent frictional adhesion in natural and synthetic gecko setae. *Journal of the royal society interface*, 7(43), 259-269.
- [55] Wu-Bavouzet, F., Cayer-Barrioz, J., Le Bot, A., Brochard-Wyart, F., & Buguin, A. (2010). Effect of surface pattern on the adhesive friction of elastomers. *Physical Review E*, 82(3), 031806.
- [56] Landau, L.D., Lifshitz, E.M., 1959. *Theory of Elasticity*. Pergamon, London
- [57] Johnson, K. L., (1987). *Contact mechanics*. Cambridge university press.
- [58] H. B. Callen, *Thermodynamics and an Introduction to, Thermostatistics*, John Wiley & Sons Inc., USA, ISBN Q-471-86256-8, 1985.
- [59] G. Carbone, L. Mangialardi, *Contact Mechanics, Adhesion and Friction of Rubber Materials*, in *Advances in Contact Mechanics: Implications for Materials Science, Engineering and Biology 2006*, editors Renato Buzio and Ugo Valbusa, pp. 145-211, Transworld Research Network, 37/661 (2), Fort P.O., Trivandrum-695 023, Kerala, India, ISBN-13: 978-8178952215, ISBN-10: 8178952211.